International Research Journal of Earth Sciences ISSN 2321–2527
Vol. **3(10),** 7-13, October **(2015)** *Int. Res. J. Earth Sci.*

Radar Observations of Equatorial Ionospheric Irregularities

Chapagain N.P.
Department of Physics, Patan Multiple Campus, Patangate, Lalitpur, Tribhuvan University, NEPAL

Available online at: www.isca.in, www.isca.me
Received 20th September 2015, revised 2nd October 2015, accepted 24th October 2015

Abstract

Long-term data set of radar observations using coherent and incoherent scatter radar sources during 1996-2008 were used to study the trend of low-latitude ionospheric irregularities, also referred to as equatorial spread F (ESF), near geomagnetic equator over Jicamarca, Peru (12°S, 76.9°W, geomagnetic latitude 1°N). Radar signatures are classified on the basis of their structures. The occurrences of radar signatures of the F-region plasma irregularities are highly seasonal and solar cycle dependence. Irregularities are more dominant during December solstice with ~88% of the total night of observations, while the irregularities occurrences are minimum during June solstice with~29% of the total nights of observations. Using incoherent scatter radar observations, the relationships of vertical drift velocities of plasma with the onset of ESF have been studied. Generally, the strong spread F develops for the early night higher upward drift velocity, while the weak spread F is most often generated for the small upward drift velocity in the early evening hours. Radar plumes or broad spread F are not developed for the early night downward drifts of plasma during the equinox season, while during the December solstice such early night downward drift inhibits the development of ESF. However, in June solstice, small upward or downward drift velocities also lead to the development of weak spread F.

Keywords: Ionospheric irregularities, equatorial spread F(ESF), radar plume, equatorial plasma bubble, plasma drifts.

Introduction

The Earth's ionosphere extending in the altitude ranges of 200-1000 km, referred to F-region ionosphere, most often shows nighttime plasma instability in the equatorial region. This post-sunset phenomenon is generally referred to as plasma irregularity or equatorial spread F (ESF) or plasma depletion or equatorial plasma bubble (EPB). The plasma irregularities at the F-region ionosphere are predominantly a nighttime phenomenon and this is a region of greatest interest to space scientists because of the complex dynamical phenomena and instability occurrence in this region. These plasma irregularities are generally magnetic field aligned with zonal widths of usually a few tens of kilometers. They extend along the magnetic field lines for hundreds to thousands of kilometers, which depend on the peak altitude of the irregularity development (EPB), while their vertical heights range from a few tens of kilometers to several hundred kilometers[1,2]. Development of such night time ionospheric irregularities in the equatorial F-region can significantly affect low-latitude navigation and communication systems.

These irregularities have been extensively studied over the past several decades[3-5]. Onospheric irregularities were first reported by scientists using HF (High-Frequency) radio ionospheric sounding experiments that took place about seven decades ago[6]. Radar techniques have been used since the commencement of space age in 1950s to study the ionosphere[3]. *Woodman and LaHoz* used radar observations from Jicamarca, Peru, and reported plume-like structures extending to high altitudes[7]. In addition to the ionosonde and radar observations[3], the plasma irregularities (or EPBs) have been detected by satellite[8], rockets[9] as well as other ground-based optical instruments[10-14].

Extensive studies of ionospheric irregularities using radar observations from Jicamarca Radio Observatory (JRO), Peru (12°S, 76.9°W, and geomagnetic latitude 1°N) have been performed since 1970. The first description of the characteristics of spread F structure observed with the Jicamarca radar observations were reported by Woodman and LaHoz[7]. According to *Hysell and Burcham,* the radar echoes observed with JULIA (Jicamarca Unattended Long-term Investigations of the Ionosphere and Atmosphere) radar observations were classified as: i. bottom typelayers, ii. bottom side layers, and iii. radar plumes[15,16]. Bottom type layers are relatively weak and narrow scattering layers in the lower F-region ionosphere with thickness less than~50 km. Bottom side layers are broader, more structured and stronger scattering layers which extends relatively higher altitudes lasting for a few hours. Radar plumes (also referred to as topside layers), which are deep, larger-scale elongated structures originating from bottom side layers and extending to the topside ionosphere[15]. *Chapagain et al.* have also reported the climatology of post sunset equatorial ionospheric irregularities using the long-term radar observations from Jicamarca, Peru[5]. They discussed the seasonal and solar cycle variations of initial altitudes and initial times of the spread F. They also revealed onset altitudes and times of radar plumes and their connections with the vertical drift velocities of the plasma.

In this study, long-term Jicamarca coherent and incoherent scatter radar observations from 1996 to 2008 have been used. We classify the radar signatures from Jicamarca radar observations as non-spread F, weak spread F, and strong spread F. The strong spread F includes both broad spread F and radar plumes. Furthermore, we analyze the seasonal and solar cycle trends of these structures associated with ESF. We also study the relationships of vertical velocities of plasma drifts with onset of ESF with seasonal and solar cycle variations using extensive data set of incoherent scatter radar observations.

Material and Methods

The JULIA radar is a low power transmitter of frequency 50 MHz.It consist of a PC- based data acquisition system with multiple receivers and makes use of the exciter stage of the Jicamarca incoherent scatter radar (ISR) to drive the main antenna array. JULIA demonstrates how the large-aperture arrays of the community's incoherent scatter radars remain useful when ISRs themselves are not running[15]. JULIA data and incoherent scatter data can be interactively retrieved through the World Wide Web.

Figure 1 shows a map of South America, exhibiting the location of Jicamarca Radar Observatory (JRO) at Jicamarca, Peru. Solid horizontal line in the figure represents the geographical equatorial line, while the dash-line plots geomagnetic latitude. It shows that Jicamarca radar observation lies near the geomagnetic equator. Radar antenna arrangement in JRO is also shown in the figure in the bottom (in rectangular box).

In this study, we have used extensive F-region coherent (JULIA) and incoherent scatter radar observations over Jicamarca, Peru, during 1245 nights from August 1996 to December 2008. Coherent and incoherent scatter radar measurements of equatorial spread F are revealed in format of range time intensity (RTI) plot, in which backscatter power is plotted against altitude and time. These RTI plot report the randomness of equatorial spread F and give the altitude and time at which the irregularities occur.

We use radar echoes from incoherent scatter radar measurements to estimate the vertical drift velocities. For this study, radar measurements were typically made over an altitudinal range of ~200-900 km with an altitudinal resolution of 50 km and temporal resolution of 5 min. The vertical velocities of the plasma drift measured by incoherent scatter radar generally taken to heights ranges from about 300 to 500 km, where the signal to noise ratios, which measures the irregularities of the ionosphere, are more pronounced, and have an accuracy of about 1-3 m/s.

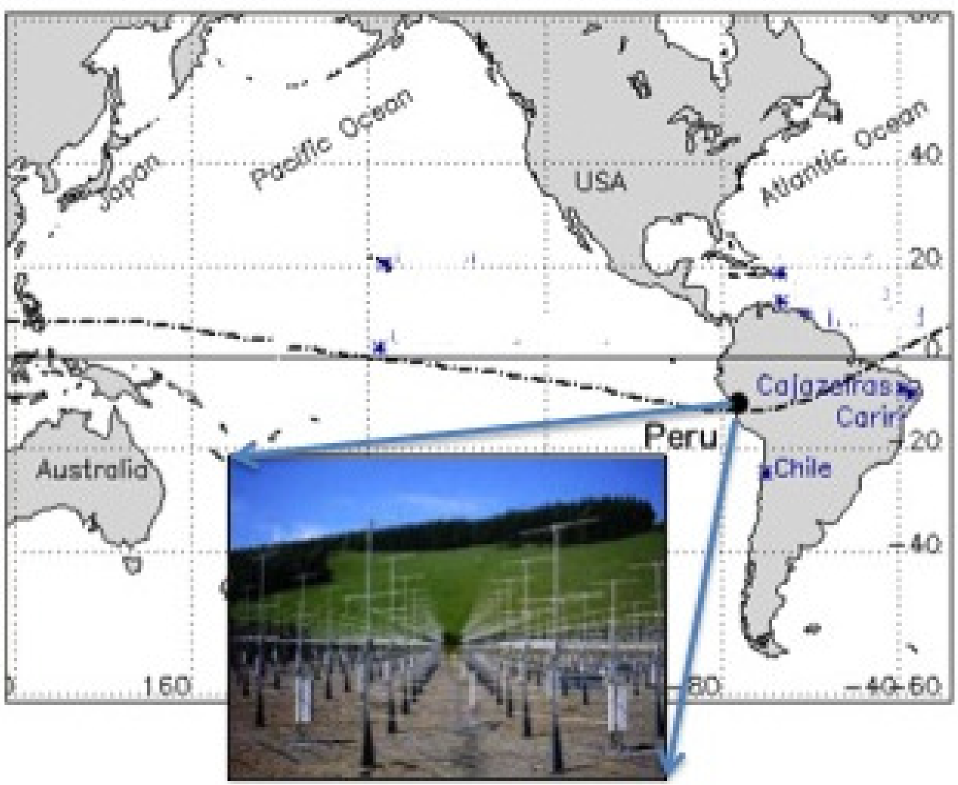

Figure-1
Map shows the location of Jicamarca Radar observatory (JRO) at Jicamarca, Peru. Arrangement of radar observations is also shown in the bottom part in rectangular box

Results and Discussion

Classification of Radar Signatures: Radar signatures associated with ESF obtained from Jicamarca radar measurements are classified according to the thickness of the structures and behavior of their propagation as followings:

Non Spread F (NSpF): If no signature in radar echo is recorded in the range time intensity (RTI) plot in the F-region ionosphere (altitude above 200 km), it is classified as non-spread F (as shown in figure-2). It illustrates that no plasma irregularity is developed as measured inside the radar antenna's field of view. The non-spread F signatures were mostly observed during the June solstice (May-August) season.

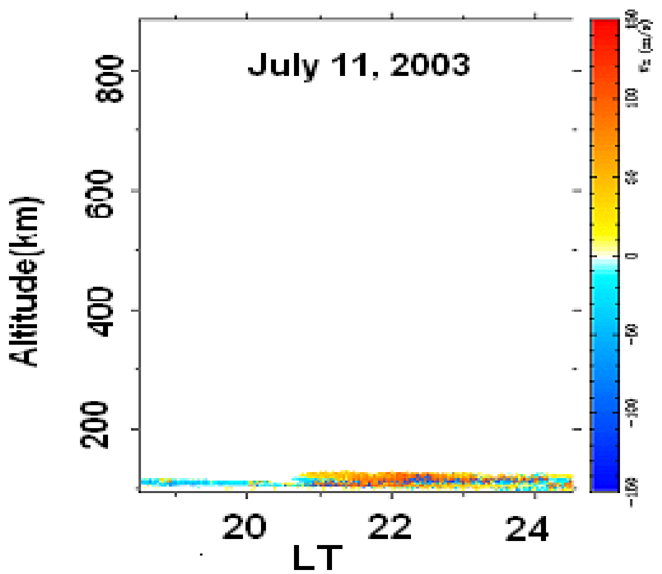

Figure-2
Non spread F as no radar signature is observed in F-regions ionosphere.

Weak Spread F (WSpF): The narrow weak layers of thickness less than about 100 km observed in range time intensity plot of radar echo are categorized as weak spread F (WSpF). These are bottom type layers[15] or undulations including the weak plumes (plumes of altitude range less than about 200km). In general, these types of irregularities are occurred in the low altitude range. An example of WSpF is shown in figure-3. The vertical bar index represents the horizontal drift velocity of the plasma inside the radar echo. Here negative value (with blue color) represents west-ward velocity of the plasma drifts, while the positive value (with red color) represents in the eastward drifts velocity of the plasma. Figure-3 also shows that the velocities of the plasma in the radar signatures have either small eastward or westward plasma drift velocities. These structures have characteristics of bottom type irregularities[14].

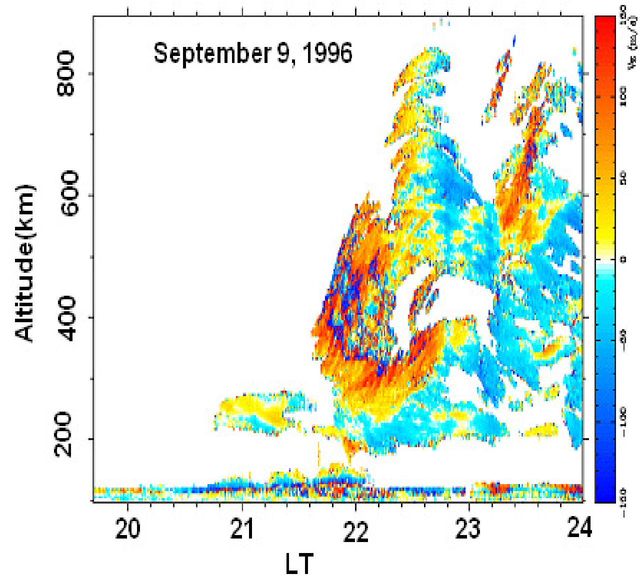

Figure-3
Example of radar signature of weak spread F over Jicamarca, Peru

Broad Spread F (BSpF): Broad and wide structured layer of thickness greater than 200km, and the temporal scale more than around 2 hours continually occurring, is classified as broad spread F (BSpF). Strong bottom side layers are of this category[15]. The typical example of broad spread F observed on September 9, 1996 is shown in figure-4. The drift velocities of plasma inside the radar signatures shown strongly eastward in early evening hour and then mostly west-ward as the night progresses.

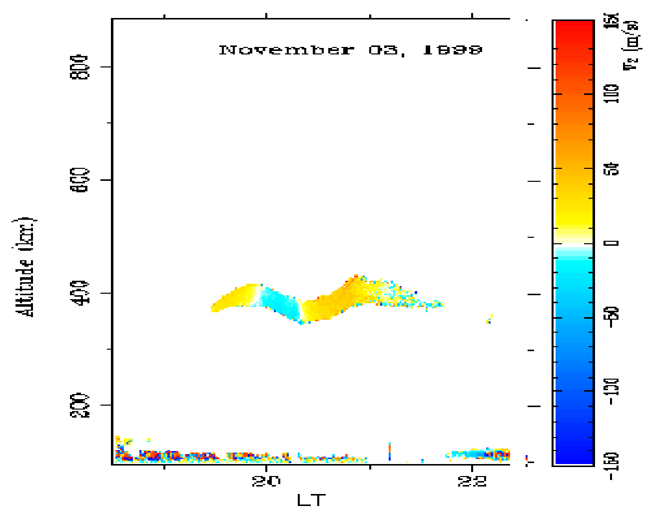

Figure-4
Example of Broad spread F radar signature over Jicamarca, Peru

Radar Plumes (RP): Rader plumes are characterized as the elongated large-scale deep plasma depletions structures that originate through the bottom side of the ionosphere and break through to the topside of the ionosphere and ascend speedily to higher altitudes. The structure originating from lower layers, which extend to the altitude range of greater than 200 km(i.e. ΔH > 200 km), are termed as radar plume as shown in figure-5, where Δ His altitude from the top of the layer from which plume generates to the peak of the plume. Figure 5illustrates an example of a radar plume occurrence during moderate solar flux condition on September 12, 2002.

Strong Spread F (SSpF): Strong structures of radar echoes are always associated with broader scattering layers extending at higher altitudes[7,15]. In our study, we consider the equatorial spread F to be strong enough when unstable layers cover altitudinal ranges in excess of 100 km. The radar plumes as well as BSpF are grouped in Strong Spread F (SSpF).

We have further grouped the data on different seasons as: i. Equinox for the months of March, April, September and October; ii. December-Solstice for the months of November, December, January and February; and iii. June-Solstice for the months of May, June, July and August in order to study the seasonal changes of radar echoes. Table-1 summarizes the frequencies of occurrences of the different types of equatorial spread F as well as the frequencies of occurrences of non spread F during three seasons using the long-term data set obtained during 1996-2008.

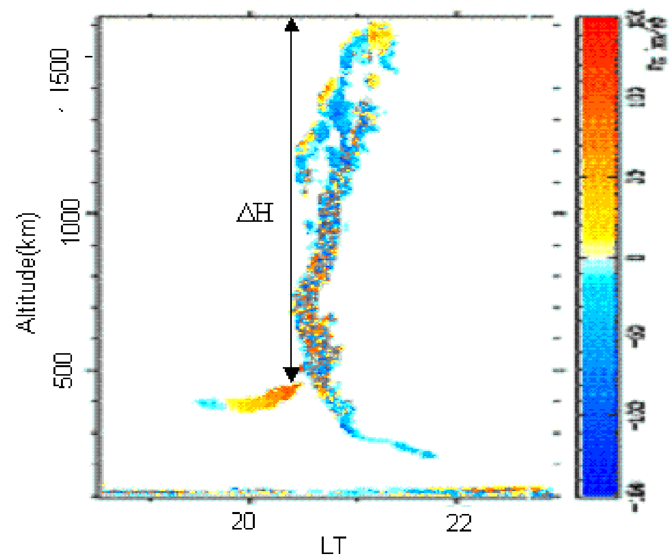

Figure-5
An example of radar plume over Jicamarca, Peru

Table-1
Statistics of ESF occurrences from Jicamarca radar observations during 1996-2008

Radar signature	**Equinox**		**December-solstice**		**June-solstice**	
	Number	**%**	**Number**	**%**	**Number**	**%**
NSpF	107	20.2	53	12.0	194	71.6
WSpF	166	31.3	199	44.8	42	15.5
Plumes	232	43.8	134	30.2	25	9.2
BSpF	*25*	4.7	58	13.0	10	3.7
Total	530		444		271	

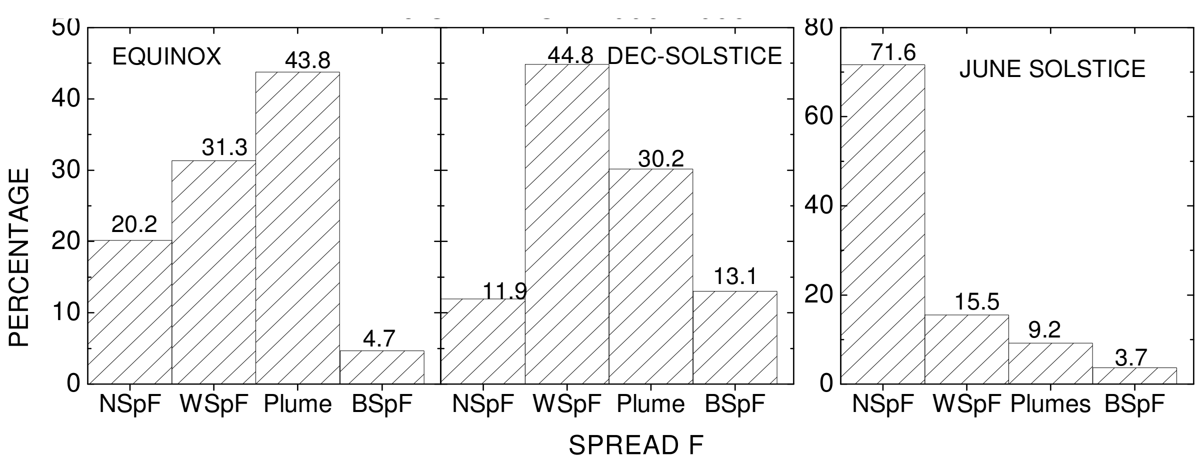

Figure-6
The relative occurrences (in %) of equatorial spread F from Jicamarca radar observations from 1996 to 2008

The relative occurrences of the radar signatures are plotted in the bar diagram as shown in figure-6. Result shows that the signatures of F-region ionospheric irregularities or equatorial spread F are seasonal dependence and shows the following features: i. In Equinox, irregularities are occurred about 80% of the total nights of observations, in which plumes are recorded at maximum of ~44% of total nights of observations. In this season, the broad spread F(BSpF) is minimum (~5%) and the weak spread F structure is moderate with a 31% of total nights of observations. ii. In December Solstice, irregularities occur about 88% of the total nights of observations. Weak spread F occurrences are maximum with a ~45% of total nights of observations, while the occurrences of plumes are ~30%, which is smaller compared to that in equinox period. The broad spread F events are larger during the December solstice (~13%) compared to the other seasons. iii. During June solstice, occurrences of irregularities are only of about 29% of the total nights of observations. In other words, ~71% of total nights of observations, no plasma irregularities are observed. Occurrences of plumes and broad spread F are only ~9% and ~4% of total nights of observations, respectively.

The results clearly show that the occurrences of ionospheric irregularities are strongly seasonal dependent with maximum during December solstice and minimum in June solstice. In southern hemisphere, December solstice is summer season, while June solstice is winter season. Therefore, the occurrences of ionospheric irregularities are maximum in summer and minimum in winter.

Vertical Velocity of Plasma Drift: We also use extensive data set of F-region incoherent scatter radar observations over Jicamarca, Peru in order to study the relationship of vertical drift velocities of plasma with occurrences of ionospheric irregularities. Our database for velocity estimation consists of over 150 days from August 1996 to December 2008. The observations were typically made between altitudes ranges of about 200 km and 900 km. The plasma drift velocities are estimated from about 300–500 km altitudes, where signal to noise ratios are significantly large. The accuracy of the plasma drift velocity estimations is typically up to ±5 m/s.

The drift velocity of the plasma is upward during daytime, and it reverses downward after sunset. The vertical plasma drift velocity just before onset of ionospheric irregularities is termed as initial vertical drift velocity or onset velocity of ESF. The upward vertical velocities of the plasma become peak just right before it start to reverses downward. This peak upward drift velocity is called prereversal enhancement drift velocity. The drift velocities of the plasma were obtained from incoherent scatter radar observations within the time period of ±5 min of onset of ESF as well as at the onset height of ionospheric irregularities.

Figure-7 illustrates the seasonal as well as solar cycle dependency of the initial vertical drift velocity of the plasma prior to the onset of weak and strong spread F with ensuing the radar plumes development. In the plot, positive values correspond to upward drift velocities; while negative values represent the downward plasma drift velocities. The post-sunset vertical drift velocities right after sunset are plotted. It should be noted that these onset velocities of the ionospheric irregularities are not necessarily directly related to the perceived ESF events, as these irregularities signatures could have been produced outside the field of view of the radar beam.

Figure-7 also reveals the large variability of the plasma drift velocities, especially during the equinox season near solar minimum conditions. Generally, higher upward vertical velocity leads to the growth of either radar plumes and broad spread F (e.g., strong spread F), while small upward velocity most often generate the weak spread F. In case of weak spread F, the drift velocities become maxima up to 30 m/s in equinox and December solstice as well. However, in case of strong spread F, the velocities range up to 60 m/s. In December solstice for weak spread F, the velocity ranges between 10 and 30 m/s.

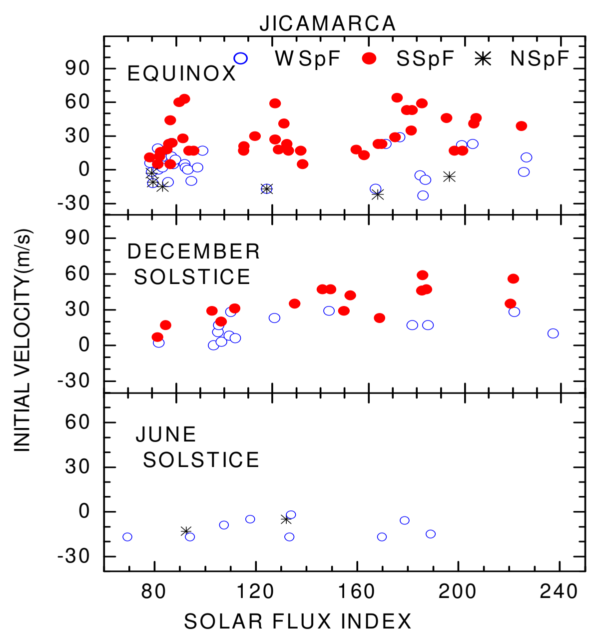

Figure-7
Seasonal and solar cycle variations of initial vertical drift velocities for different types of radar echoes

Results also illustrate that downward drifts do not lead to the development of strong spread such as radar plumes or broad spread F during the equinox. Instead, such downward drifts inhibit the development of spread F in the December solstice. In June solstice, it is seen that vertical drift velocities are either small upward or downward leading to the development of weak spread F. Non-spread F appears as the initial vertical velocity is downward. If the velocity is small (<10 m/s) or negative, the weak spread F occurs. Hence the contribution of vertical velocity for generation and evolution of ESF are solar cycle as well as seasonal dependent.

We examine relationships of initial vertical drift velocity and prereversal velocity enhancement for occurrences weak and strong spread F in equinox and December solstice as shown in Figure 8. The small circles correspond to the spread F events during the low solar flux (<120) conditions, while the big circles correspond to the spread F events during high solar flux (>120) conditions. Results illustrate that prereversal velocity enhancement is always greater than the initial vertical plasma drift velocity for the spread F to be occurred. When both the initial vertical velocities and prereversal velocities enhancements are large, the strong spread F occurs. The main feature of Figure 8 is in good agreement with the prereversal velocity enhancement presented by *Fejer et al.*[17], who drew similar conclusion on the basis of long-term Jicamarca incoherent scatter radar observations during 1968 - 1992. Our results also illustrate that the weak spread F can occur even if the initial drift velocities near dusk are downward provided that the prereversal velocities enhancements are positive, which matches well with the previous results reported by Fejer et al.[17], Rodrigues et al.[18]andAdebesin et al.[19].

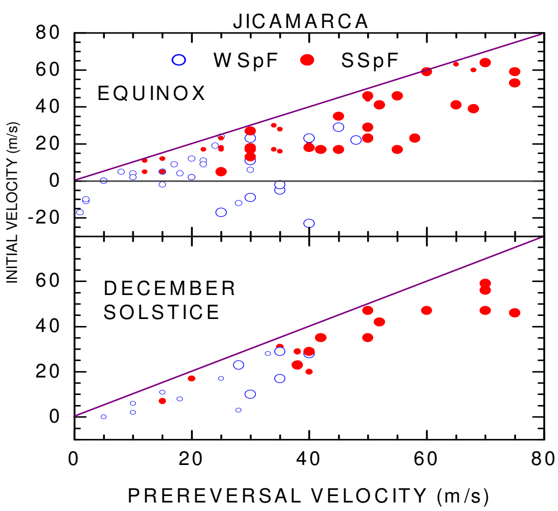

Figure-8
The relationships between initial vertical drift velocity and prereversal enhancement velocity during equinox and December Solstice

Conclusion

This study reports the long-term coherent and incoherent scatter radar observations of post-sunset equatorial spread F over Jicamarca from August 1996 to December 2008. We classified the radar signatures as non-spread F, weak spread F, broad spread F, and radar plume. The results clearly reveal that the occurrences of ionospheric irregularities are strongly seasonal dependent with maximum rate of occurrences during the December solstice (occurrences of ~88% of total nights of observations), and the minimum occurrences during June solstice (~29% of total nights of observations). This illustrates that ionospheric irregularities occur maximum in summer and minimum in winter seasons.

We also study relationships between vertical drift velocities of plasma with the onset of equatorial spread F using incoherent scatter radar observations. The results show that higher upward vertical plasma drifts leads to the development of strong spread F, while the small upward velocity most often generate the weak spread F. The downward drifts in the early night do not lead to the development of strong spread F such as radar plumes and broad spread F during the equinox; instead it inhibits the development of spread F in December solstice. In June solstice, it is seen that vertical drift velocities are either small upward or downward leading to the development of weak spread F or non-spread F. In addition, the prereversal vertical drift peaks are good correlated with initial vertical velocity of plasma, which are primarily responsible for the development of ionospheric irregularities or equatorial spread F.

Acknowledgments

I would like to thank the team of the Jicamarca Radio Observatory for providing the data for this study.

References

1. Sobral J.H.A., Abdu M.A., Takahashi H., Taylor M.J., de Paula E.R., Zamlutti C J., de Aquino M.G., and Borba G.L., Ionospheric plasma bubble climatology over Brazil based on 22 years (1977–1998) of 630 nm airglow observations, *J. Atmos. Terr. Phys.,* **64**, 1517–1524 **(2002)**

2. Chapagain N.P., Taylor M.J., and Eccles J.V., Airglow observations and modeling of F region depletion zonal velocities over Christmas Island, *J. Geophys. Res*., **116**, A02301, doi:10.1029/2010JA015958**(2011)**

3. Farley D.T., Basley B.B., Woodman R. F. and McClure J. P., Equatorial spreadF: Implications of VHF radar observations, *J. Geophys. Res.,* **75**, 7199 –7216 **(1970)**

4. Fejer B.G. and Kelley M.C., Ionospheric irregularities, *Rev. Geophys.,***18**, 401-454 **(1980)**

5. Chapagain N.P., Fejer B.G, and. Chau J.L., Climatology of post-sunset equatorial spread F over Jicamarca, *J. Geophys. Res.,***114,** A07307, doi:10.1029/2008JA013911 (**2009**)

6. Kudeki E., Akgiray A., Milla M., Chau J.L. and. Hysell D.L, Equatorial spread F initiation: Post-sunset vortex, thermospheric winds, gravity waves, *J. Atmos. Sol.-Terr. Phys.,* 69, 2416– 427 **(2008)**

7. Woodman R. F., and LaHoz C., Radar observations of F-region equatorial irregularities*, J. Geophys. Res.,* **81**, 5447–5466 **(1976)**

8. Gordon W.E., Incoherent scattering of radio waves by free electrons with applications to space exploration by radar, *Proc. IRE,* 46, 1824 (**1958**)

9. McClure J.P., Hanson W.B., and Hoffman J.H., Plasma bubbles and irregularities in the equatorial ionosphere*, J. Geophys. Res.,* 8, 2650 **(1977)**

10. Kelley M.C., Pfaff R., Baker K.D., Ulwick J.C., Livingston R., Rino C. and Tsunoda R., Simultaneous rocket probe and radar measurements of equatorial spread F – transitional and short wavelength results, *J. Geophys. Res.,* **87**, 1575 **(1982)**

11. Weber E.J., Buchau J., Eatther R.H. and Mende S.B., North-south aligned equatorial airglow depletions, *J. Geophys. Res.,* **83**, 712–716 **(1978)**

12. Mendillo M. and Baumgardner J., Airglow characteristics of equatorial plasma depletions, *J. Geophys. Res.,* **87**, 7641–7652 **(1982)**

13. Taylor M. J., Eccles J.V., LaBelle J. and. Sobral J.H. A, High resolution OI (630 nm) image measurements of F-region depletion drifts during the Guára campaign, *Geophys. Res. Lett.,* **24,** 1699–1702 **(1997)**

14. Makela J.J. and Otsuka Y., Overview of NighttimeIonospheric Instabilities at Low- and Mid-Latitudes: Coupling Aspects Resulting in Structuring at the Mesoscale", *Space Science Reviews*, **168**, Issue 1, 419-440 **(2012)**

15. Hysell D.L. and Burcham J.D., JULIA radar studies of equatorial Spread F, *J. Geophys. Res.,***103**, 29,155–29,167 **(1998)**

16. Hysell D.L., An overview and synthesis of plasma irregularities in equatorial spread F, J. *Atmos. Sol.-Terr. Phys.,* **62,** 1037-1056 **(2000)**

17. Fejer B.G., Scherliess L. and de Paula E.R., Effect of the vertical plasma drift velocity on the generation and evolution of equatorial spread F, *J. Geophys. Res.*, **104**, 19, 859 –19,869 **(1999)**

18. Rodrigues F., Smith J., Milla M. and Stoneback R., Daytime ionospheric equatorial vertical drifts during the 2008–2009 extreme solar minimum, *J. Geophys. Res.*, **120(2),** 1452–1459, doi:10.1002/2014JA020478 **(2015)**

19. Adebesin B., Adeniyi J., Adimula I., Oladipo O., Olawepo A. and Reinisch B., Comparative analysis of nocturnal vertical plasma drift velocities inferred from ground -based ionosonde measurements of hmf2 and hf, *J. Atmos. Sol.-Terr. Phys.,* **122(0),** 97–107, doi:10.1016/ j.jastp. 2014.11.007 **(2015)**